Supporting information

Threonine: A Universal Single-Molecule Bifunctional Modifier Boosting for Efficient and Stable Perovskite Solar Cells and Modules

Qinxue Wang,[a] Yu Wang,*[a] Chu Zhang,[a] Jiaxing Song,*[b] Luping Lyu,*[c] Qingping Tang,[d] Guoqing Li,[d] Zaifang Li[b] and Tingli Ma[e]

[a] College of Materials and Chemistry, China Jiliang University, 258 Xue Yuan Street, Qiantang District, Hangzhou, Zhejiang 310018, PR China

[b] Zhejiang Key Laboratory of Advanced Tandem Photovoltaic Technology, College of Biological and Chemical Engineering, Jiaxing University, Jiaxing, Zhejiang, 314001, PR China

[c] Hangzhou Polytechnic University, Hangzhou, Zhejiang, 310018, PR China

[d] Jiaxing Daze Photoenergy Co.Ltd Xiuzhou District, Jiaxing, Zhejiang, 314031, PR China

[e] Graduate School of life Science and Systems Engineering, Kyushu institute of Technology, 2-4 Hibikino, Wakamatsu, Kitakyushu, Fukuoka 808-0196, Japan

Corresponding author:

wangyu19920924@cjlu.edu.cn

songjx@zjxu.edu.cn

mailofllp@126.com

The energy levels could be calculated with the following equations 1:[1]

$E_{\mathrm{HOMO}} = 21.22 - (E_{\mathrm{cutoff}} - E_{\mathrm{onset}})$

$E_{\mathrm{g}} = E_{\mathrm{LUMO}} - E_{\mathrm{HOMO}}$

E_g, E_{HOMO}, E_{LUMO}, $E_{cut\text{-}off}$, E_{oneset} represent the bandgap, highest occupied molecular orbital, lowest unoccupied molecular orbital and the ending and starting edges in the UPS spectrum, respectively

The PL decay curve is fitted using the following equation 3:[3]

$$I(t) = I_0 + A_1 e^{\frac{-t}{\tau_1}} + A_2 e^{\frac{-t}{\tau_2}}$$

Where I_0 is a constant for the baseline offset. A_1 and A_2 are the decay amplitudes, τ_1 is the rapidly decaying carrier lifetime reflecting the ability of SnO_2 to extract electrons, and τ_2 is the lifetime of slow complexation in the PVK film phase.

The average PL decay lifetime (τ_{ave}) can be obtained using the following equation 4:[4]

$$\tau_{a\ v} \overline{\overline{g}} \frac{A_1}{A_1 + A_2}\tau_1 + \frac{A_2}{A_1 + A_2}\tau_2$$

The trap state density can be calculated by V_{TFL} using the following Equation 5:[5]

$$N_t = \frac{2\varepsilon_0 \varepsilon V_{TFL}}{eL^2}$$

where ε_0 and ε are the vacuum permittivity and relative permittivity of PVK, respectively, *e* is the elementary charge, and *L* is the thickness of the PVK film.

The conductivity can be calculated by V_{TFL} using the following Equation 6:[6]

$$\sigma = \frac{k * 1000}{A * \left(d * 10^{-7}\right)^{-1}}$$

where *k*, *A* and *d* represent the slope, cell area, and transmission layer thickness (nm), respectively.

The mobility can be calculated by V_{TFL} using the following Equation 7:[7]

$$\mu = \frac{J * 8L^3}{9 * \varepsilon_r * \varepsilon_0 * V^2}$$

where *J*, *L*, ε_r, ε_0 and *V* represent the current density, layer thickness, relative permittivity of the material, permittivity of free space and voltage respectively.

The hysteresis index HI calculated by the following Equation 8:[7]

Hysteresis Index = [Power Conversion Efficiency Reverse Scan (PCERS)- Power Conversion Efficiency Forward Scan (PCEFS)]/ [Power Conversion Efficiency Reverse Scan (PCERS)

Experimental Section

Material：

Except where otherwise stated, the solvents and chemicals covered in this article is metrically available and do not require further purification. Threonine acid (Thr), formamidine iodide (FAI, 99.5%), methylammonium iodide (MAI, 99.5%), lead iodine (PbI_2, 99.99%), SnO_2 (12 wt.%) are all provided by Xi'an Polymer Light Technology. Spiro-OMeTAD (99.8%) was supplied by Shenzhen Feiming Science and Technology Co., Ltd. Sigma Aldrich provided t-BP (98%), and Li-TFSI (99.5%). Dimethylformamide (DMF, anhydrous, 99.8%),

dimethyl sulfoxide (DMSO, anhydrous, 99.7%), chlorobenzene (CB, anhydrous, 99%) are purchased from J&K. Isopropanol (IPA, anhydrous, 99.5%) is manufactured by Sinopharm Chemical Reagent Co., Ltd. The indium tin oxide is bought from Yingkou Opctech New Energy Technology Co., Ltd

Device Fabrication:

Fabrication of small area devices: ITO substrates were ultrasonically cleaned using detergent, deionized (DI) water, acetone, and isopropanol, each for 30 minutes. A SnO_2 ETL was formed by spin-coating a precursor solution at 2,000 rpm for 30 seconds and annealing at 150 °C for 30min. For devices treated with Thr, a specific amount of Thr powder was weighed to prepare a 2.5 mg/ml Thr solution. This solution was then mixed with SnO_2 at a ratio of Thr solution: SnO_2= 3:1 to complete the mixing of Thr into SnO_2. Subsequently, spin-coat the mixed SnO_2-Thr solution onto the ITO-coated glass substrate at 2000 rpm for 30 seconds, followed by annealing at 150°C for 30 minutes. The $FA_{0.9}Cs_{0.1}PbI_3$ (1 M) perovskite precursor solution was prepared by dissolving CsI, FAI, and PbI_2 (molar ratio = 0.1:0.9:1.0) into DMF and DMSO mixture solution (volume rate = 8.5:1.5). For HTL precursor solution, 90 mg Spiro-OMeTAD, 36 μL t-BP and 22 μL acetonitrile solution of Li-TFSI (520 mg/mL) were dissolved in 1 mL CB. All of the solutions were filtered through 0.45 μm syringe filter before use.

The perovskite precursor solution was spun at 1000 rpm for 10 s, followed by 5000 rpm for 30 s, and Chlorobenzene was dropped at 20 s after start. After spin-coating, the film annealed at 150 °C for 10 min to obtain the perovskite film. Then 45 μL Spiro-OMeTAD solution was coated on the film and spun at 5000 rpm for 30 s. Afterwards, HTL was prepared by mixing 72.3 mg of spiro-OMeTAD, 28.8 μL of t-BP, and 17.5 μL of Li-TFSI solution (520 mg/mL in acetonitrile) in 1 mL of chlorobenzene, followed by spin-coating at 2,000 rpm for 30 seconds. Finally, 100 nm-thick silver electrodes were deposited via thermal evaporation. The fabricated cells had effective areas of 0.06 cm^2. The J-V tests are conducted in N_2.

Preparation of modules:

Rigid PSCs: The 10*10 cm glass/ITO rigid substrates (15 Ω/sq, Advanced Election Technology Co., Ltd.) were etched and sequentially washed with detergent, deionized water, ethanol and isopropanol in an ultrasonic bath for 10 min.

Flexible PSCs: The PEN/ITO flexible substrates (40 Ω/sq, Peccell Technologies, Inc.) were etched and sequentially washed with detergent, deionized water, ethanol and isopropanol in an ultrasonic bath for 10 min.

Then the flexible substrates were then attached onto rigid substrates covered with PDMS for surface flatness and treated with ultraviolet ozone for 15 min before SnO_2 deposition.

Fabrication of modules:

The solar module, with an active area of 52.8 cm^2, was fabricated on PEN/ITO and glass/ITO. The solar module comprising 11 subcells was fabricated using P1, P2, and P3 laser scribing lines with a wavelength of 1064 nm. The pre-patterned ITO substrates were pre-scribed with P1 lines (approximately 200 μm wide), followed by cleaning with acetone and isopropanol to remove adhesive residues. The preparation method for the ITO/SnO_2 substrate is the same as that for the small-area devices. For perovskite deposition, the precursor solution was dispensed ahead of the blade and coated at 20 mm/s. The wet film was immediately treated with flash evaporation for 38 seconds to accelerate solvent removal. The perovskite film was then transferred to a hotplate and annealed at 100 °C for 15 minutes. The preparation of the hole transport layer (HTL) is the same as that for the small-area devices. P2 and P3 scribing lines were patterned using a 355 nm picosecond laser system. The P2 lines (approximately 100 μm wide) were achieved with an average laser power of 12 W and a pulse repetition frequency of 65 kHz. After electrode deposition, the P3 lines (approximately 80 μm wide) were patterned under an average laser power of 0.78 W and a pulse repetition frequency of 80 kHz. The spacing between P1, P2, and P3 lines was maintained at approximately 30 μm. The active area was determined to be 52.8 cm^2 by calculating the difference between the shadow mask area and the dead zone.

DFT calculations: First principles theory calculations are carried out using the Vienna Ab initio Simulation Package (VASP) within the framework of the generalized gradient approximation functional.[8-10] Projected augmented wave (PVW) potentials are used to describe the ionic cores and take valence electrons into account using a plane wave basis set with a kinetic energy cutoff of 400 eV.[11,12] K-points are sampled under the Monkhorst-Pack scheme for the Brillouin-zone integration (K-points were sampled using the Gamma Point). In all calculations, the forces acting on all atoms are < 0.02 eV/Å in fully relaxed structures, and self-consistency accuracy of 10^{-5} eV is reached for electronic loops. The surface is modeled as a periodic slab consisting of at least five atomic layers separated by a vacuum of at least 25 Å in the direction normal to the surface.[13]

The electrostatic potential of the Thr was calculated using the Gaussian 16 program (Revision C.01)[14] with the B3LYP functional[14]. All-electron 6-311+G(d,p) basis sets were applied for C, H, O, and N. Additionally, the Grimme-D3 scheme was employed to account for Van der Waals interactions. The perovskite system considered in the DFT calculations is $FACsPbI_3$, which was used as the representative PVK model in this study.

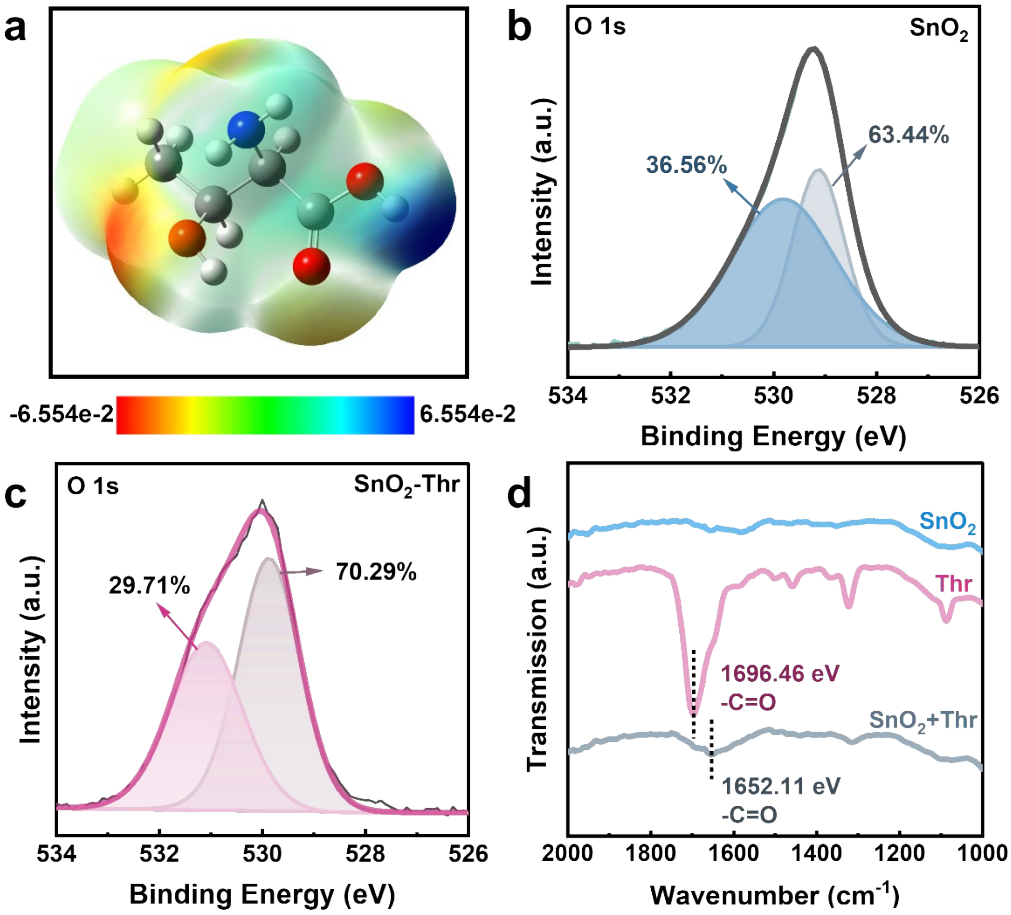

Fig. S1 a) The ESP of Thr, where red, blue, white, and gray atoms represent O, N, H, and C elements, respectively. b-c) The XPS of O1s. d) The FTIR of SnO_2, Thr and SnO_2-Thr.

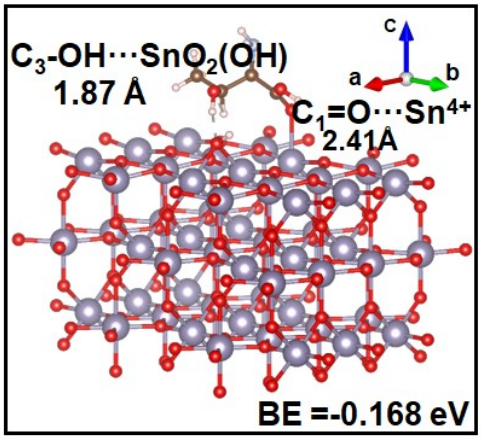

Fig. S2 DFT calculations of the binding energy perform on the binding energies of C_1=O with Sn^{4+} when SnO_2-OH bounds to C_3-OH, where the gray, brown, red, light blue and light pink represent the Sn, C, O, N and H atoms.

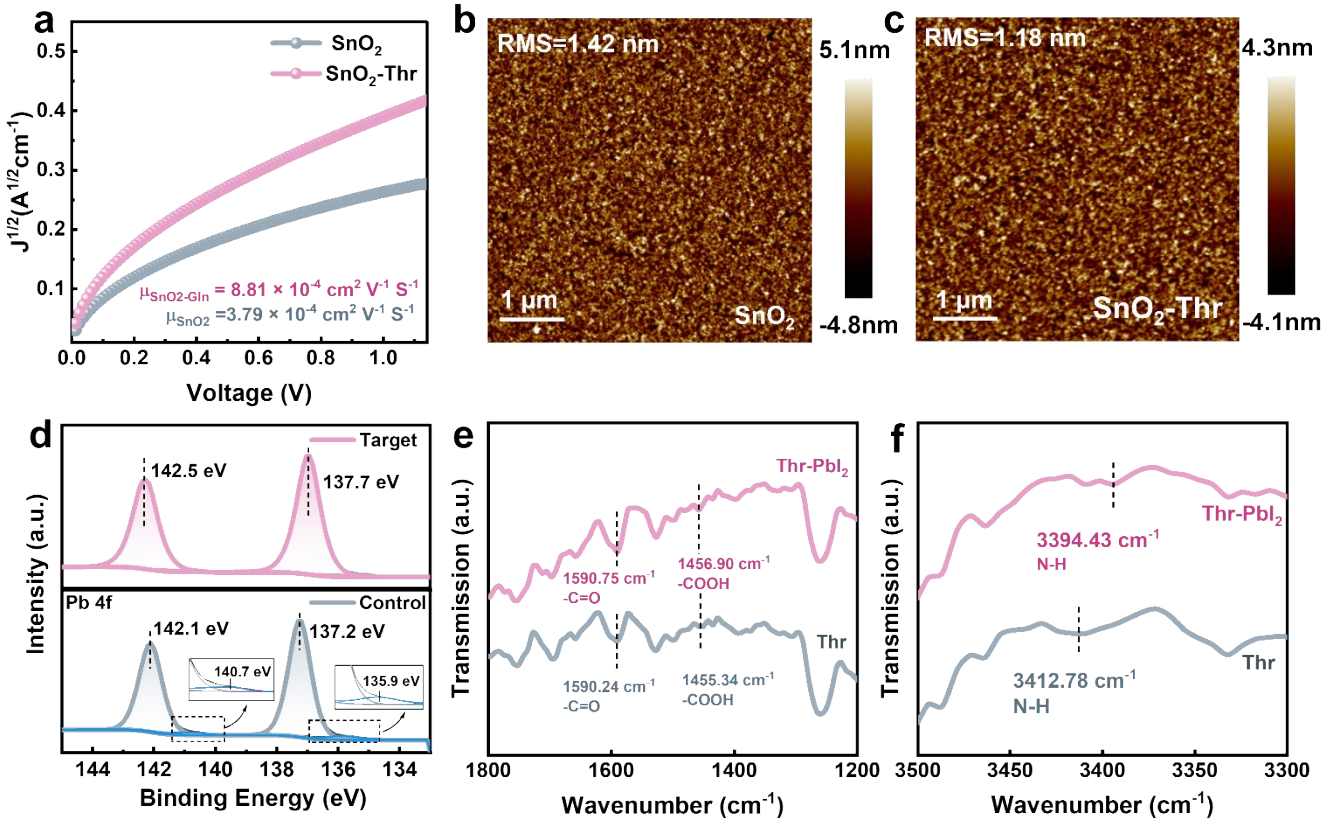

Fig. S3 a) The electron mobility of SnO_2 and SnO_2-Thr. b-c) The AFM of SnO_2 with and without Thr mixing. d) The XPS of Pb 4f. e-f) The FTIR of Thr and PbI_2-Thr.

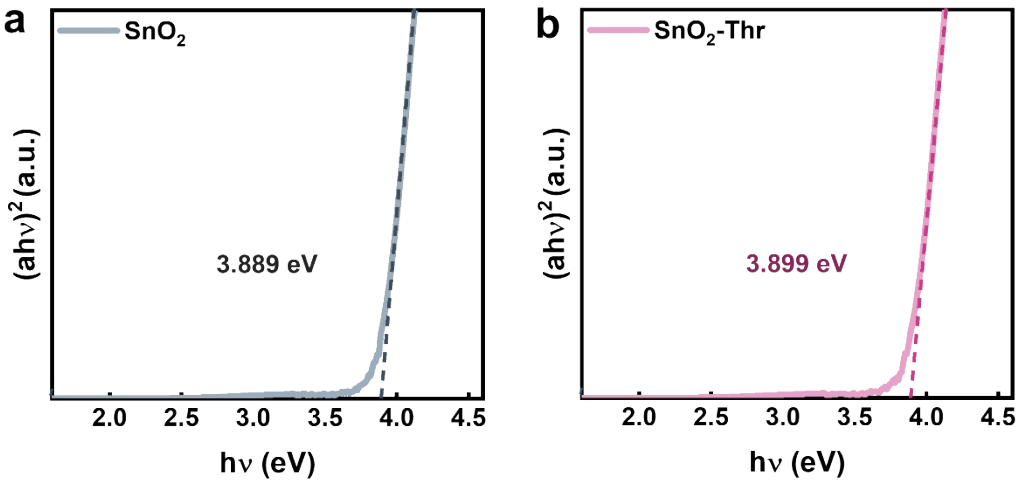

Fig. S4 a-b) The bandgap of SnO_2 and SnO_2-Thr.

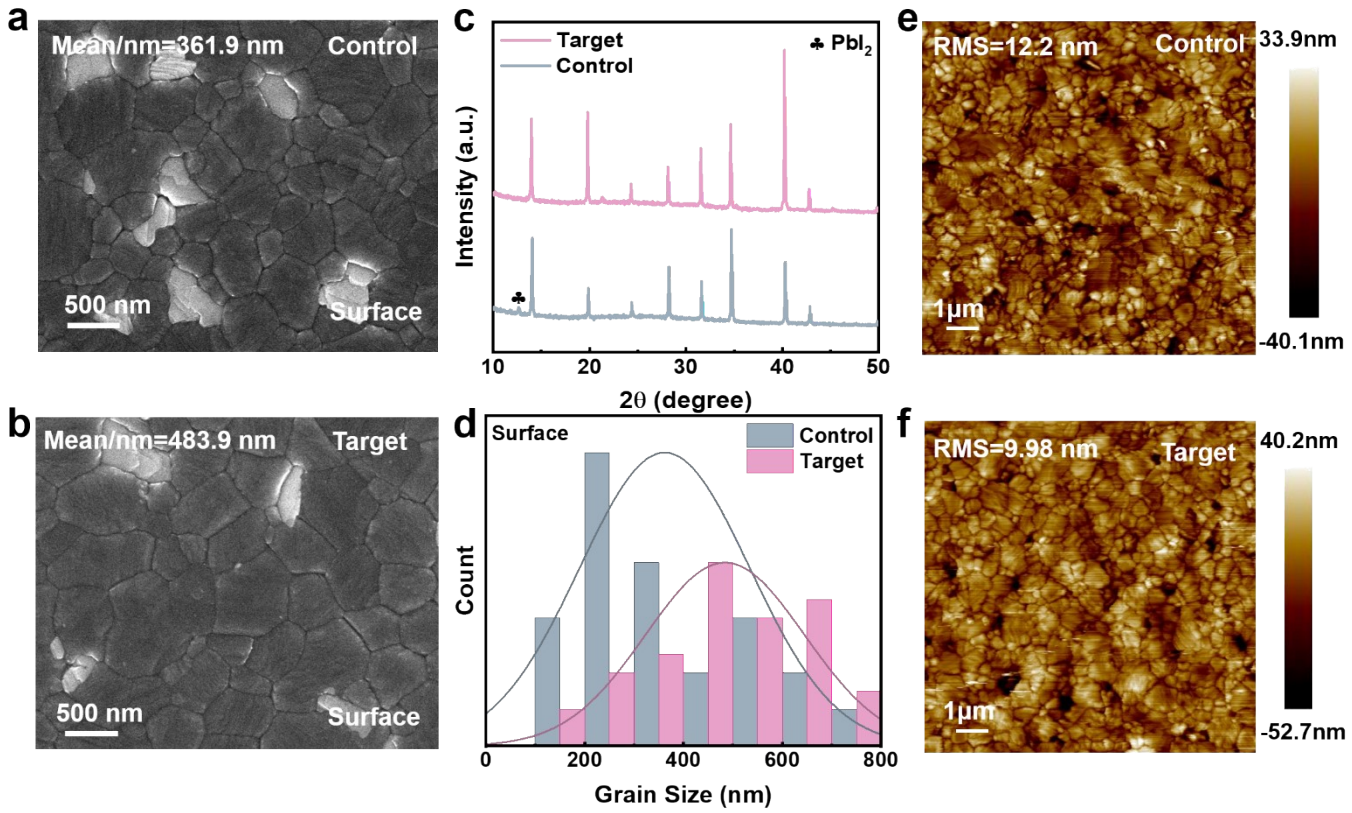

Fig. S5 a-b) The SEM of surface PVK films. c) The XRD of PVK films. d) Grain size distribution of buried and surface PVK films without and with Thr treated. The grain sizes are estimated from the SEM images by the Nano Measurer 1.2 software. e-f) The AFM of PVK with and without Thr modification.

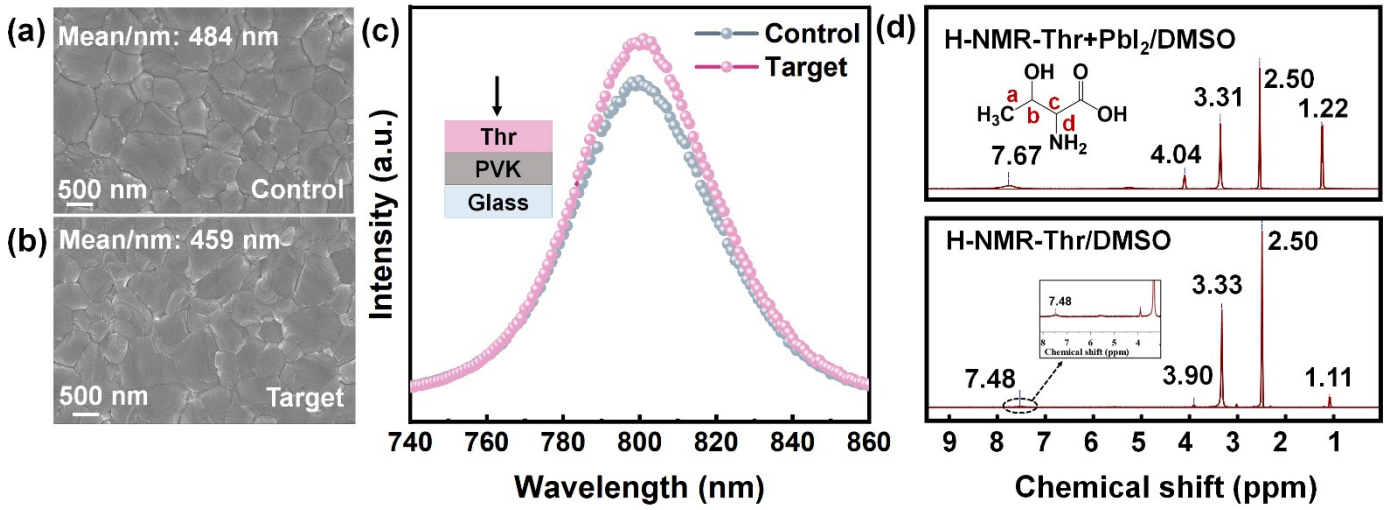

Fig. S6 a-b) The SEM of PVK films. c) The PL of Glass/PVK and Glass/PVK/Thr. (d)The NMR of Thr and Thr+PbI_2.

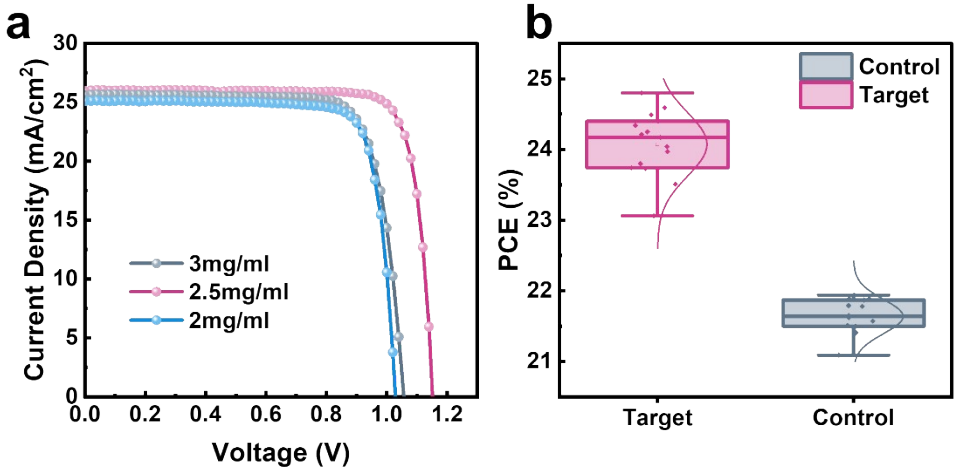

Fig. S7 a) The J-V curves of PSCs with 2mg/ml, 2.5mg/ml and 3mg/ml Thr modification. b) PCE box plot of devices before and after Thr modification.

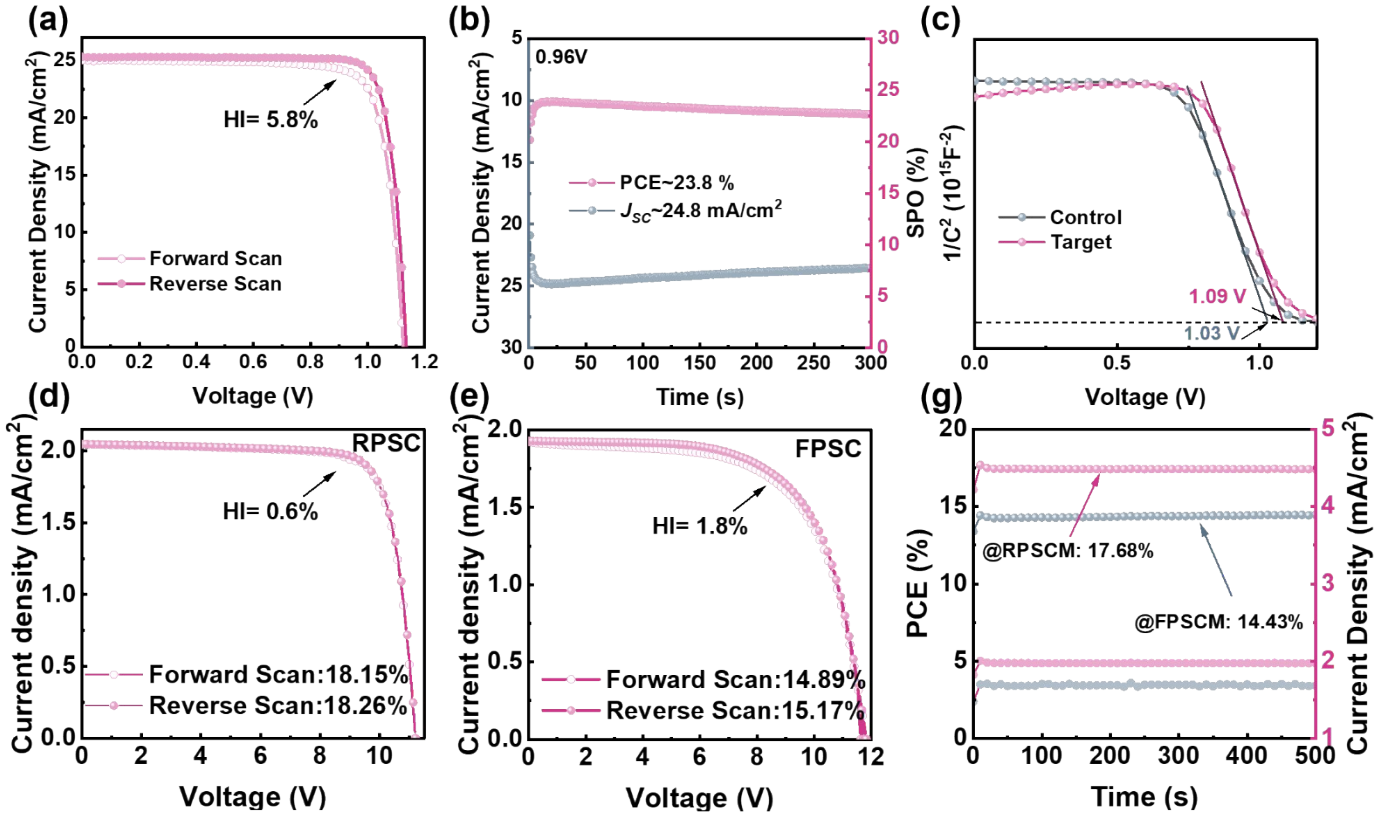

Fig. S8 a) The HI of modified device. b) The SPO of the device after modification. c)The SCLC of devices with and without modification. d-e) The HI of RPSC and FPSC. f) The steady-state efficiency of RPSC and FPSC.

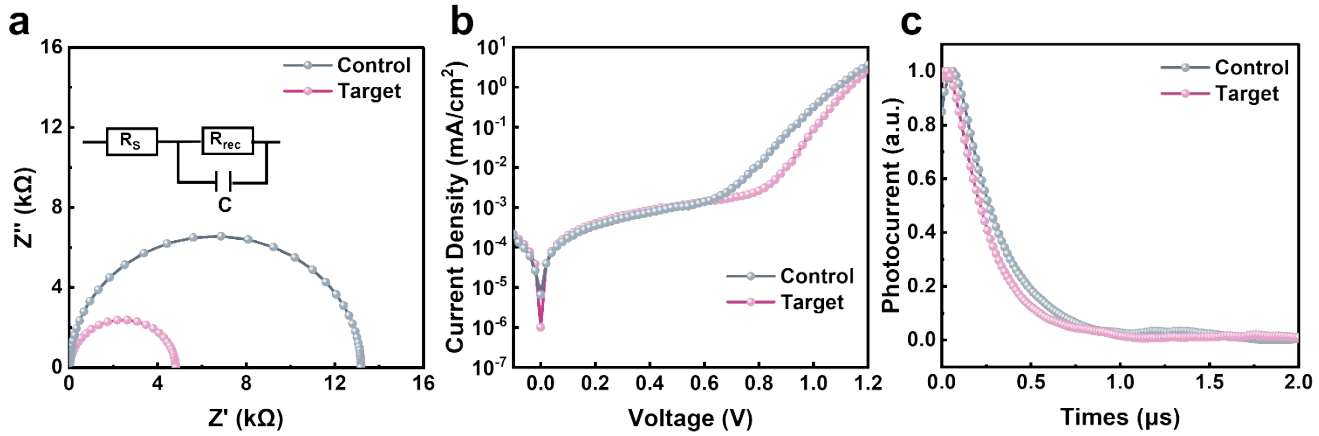

Fig. S9 a) The EIS of device with and without modification. b) The dark current of SnO_2/PVK and SnO_2-Thr/PVK. c) The TPC of devices with and without modification.

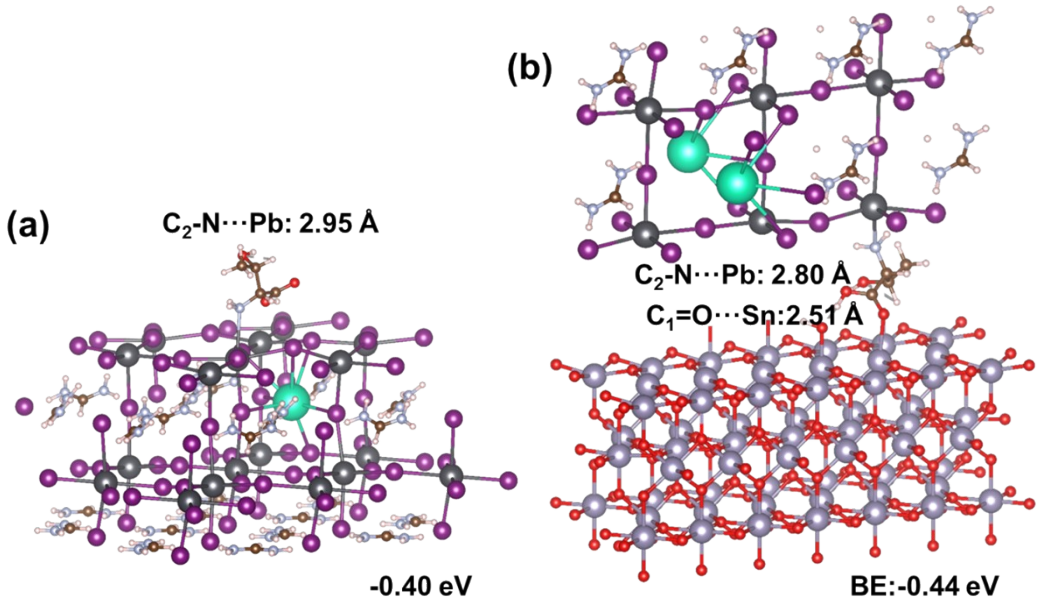

Fig. S10 a) The binding energy between Pb and the C_2–N(NH_2). (b) The binding energy between Pb and the C_2–N(NH_2) when C_1=O group is coordinated to Sn. Where the gray, brown, red, light blue, light pink, purple, black and green represent the Sn, C, O, N, H, I, Pb, Cs atoms.

Table S1. The cost of modifier

Device structure	Modifier	Price (US $)
FTO/SHA-SnO_2/PVK/ Spiro-OMeTAD /Au [15]	Sodium Hyaluronate (SHA)	46.32/g
FTO/ SnO_2/K_8SOS/PVK/Spiro-OMeTAD/Au [16]	Potassium Sucrose Octasulfate (K_8SOS)	45.9/g
FTO/ SnO_2/AMPA/PVK/Spiro-OMeTAD/Ag [17]	Aminomethyl Phosphonic Acid (AMPA)	25.27/g
FTO/ SnO_2/DLAM/PVK/Spiro-OMeTAD/Au [18]	DL-2,3-diaminopropionic acid monohydrochloride (DLAM)	5.88/g

ITO/ SnO_2/PAA/PPA/PVK/Spiro-OMeTAD/Ag [19]	3,4,5-trimethoxyphenylacetic acid	1.89/g
FTO/ SnO_2/PGA/PVK/Spiro-OMeTAD/Au [20]	Polyglutamic Acida	5.05/g
ITO/ SnO_2-CIT/ PVK/Spiro-OMeTAD/Au[21]	L-Citrulline	0.84/g
ITO/SnO_2-Glu/PVK/ Spiro-OMeTAD/Ag	glutamic acid (Glu) **This work**	**0.39/g**

Table S2. TRPL data of control and target devices.

		τ_1 (ns)	τ_2 (ns)	τ_{avg} (ns)
ITO/SnO_2/PVK	Control	30.56	189.50	142.99
	Target	36.17	105.97	80.82

Table S3. EIS data of control and target devices.

	Control (Ω)	**Target (Ω)**
R_s	40.02	39.33
R_{rec}	4769	13136

Table S4. Current PCE of larger area modules in rigid perovskite solar cells

Module area (cm^2)	**Active area (cm^2)**	**PCE (%)**	**Year**
5 cm * 5 cm [22]	10	21.02	2025
5 cm *5 cm [23]	10	20.98	2023
5 cm * 5 cm [24]	21	20.32	2025
15 cm *15 cm [25]	18.48	18.54	2025
10 cm *10 cm	52.8	18.26	**This work**
10 cm*10 cm [26]	/	18.42	2025
/ [27]	25	18.00	2024
5 cm *5 cm [28]	/	16.5	2024
10 cm *10 cm [29]	94.6	11.25	2024
10 cm *10 cm [30]		11.08	2025
2 cm*2 cm [31]	2	10.30	2024

Table S5. Current PCE of larger area modules in flexible (n-i-p) perovskite solar cells

Structure	**Active area**	**PCE**	**Year**

	(cm^2)	(%)	
PET/ITO/P-SnO_2/PVK/ Spiro-OMeTAD/Au [32]	600	16.28	2025
PET/ITO/SnO_2/PVK/Spiro-OMeTAD/Au [33]	36.50	18.71	2023
PET/ITO/SnO_2 /PVK/PEAI/Spiro-OMeTAD/Au [34]	117	17.52	2024
PET/ITO/SnO_2/PVK/Spiro-OMeTAD/Ag	52.8	15.17	**This work**
PET/TCE/SnO_2/PVK/PTAA/Ag [35]	94	14	2023
PET/ITO/SnO_2/PVK/Spiro-OMeTAD/Au [36]	16.8 21.84	12 11.7	2021
PET/IMI/SnO_2/FAPA/PVK/Spiro-OMeTAD/C [37]	20.25	11.6	2024
PET/TCE/SnO_2/PVK/HTAB/P3HT/C/Ag [38]	49.5	11	2024

Reference

1 Y. Li, B. Wang, T. Liu, Q. Zeng, D. Cao, H. Pan and G. Xing, *ACS Appl. Mater. Interfaces* 2022, **14**, 3284.

2 S. Sanghi, A. Agarwal, M. Chauhan, E. Arya, A. Kumari, S. Kaushik and P. Sharma, *Mater. Today Proc.* 2023, **82**, 79.

3 H. Zheng, D. Liu, Y. Wang, Y. Yang, H. Li, T. Zhang, H. Chen, L. Ji, Z. Chen and S. Li, *Chem. Eng. J.* 2020, **389**, 124266.

4 S. Chen, C. Zhang, Y. Ye, C. Ma, C. Wang, Q. Wang, Y. Zhao, M. Nie, L. Shi, Y. Yu, L. Gao, M. Chen, Y. Sulaiman and T. Ma, *Sol. Energy Mater. Sol. Cells* 2025, **285**, 113548.

5 Y. Wang, J. Ye, J. Song, L. Chu, Y. Zang, G. Li, Q. Zhou, G. Yang, Y. Tu, Y. Jin, Z. Li and W. Yan, *Small*, 2024, **20**, 2304273.

6 L. Wang, J. Xia, Z. Yan, P. Song, C. Zhen, X. Jiang, G. Shao, Z. Qiu, Z. Wei, J. Qiu and M. K. Nazeeruddin, *Adv. Funct. Mater*. 2022, **32**, 2204725.

7 Q. Wang, C. Zhang, C. Wang, H. Li, Y. Wu, S. Chen, L. Li, Y. Wang, M. Chen, L. Lyu, T. Ma and W. Yan, *Small*, 2025, **21**, e06991.

8 G. Kresse and J. Furthmüller, *Comput. Mater. Sci.* 1996, **6**, 15.

9 G. Kresse and J. Furthmüller, *Phys. Rev. B* 1996, **54**, 11169.

10 J. P. Perdew, K. Burke and M. Ernzerhof, *Phys. Rev. Lett.* 1996, **77**, 3865.

11 G. Kresse and D. Joubert, *Phys. Rev. B* 1999, **59**, 1758.

12 H. J. Monkhorst and J. D. Pack, *Phys. Rev. B* 1967, **13**, 5188.

13 J. J. Xue, R. Wang, K. -L. Wang, Z.-K. Wang, I. Yavuz, Y. Wang, Y. G. Yang, X. Y. Gao, T. Y. Huang, S. Nuryyeva, J.-W. Lee, Y. Duan, L.-S. Liao, R. Kaner and Y. Yang, *J. Am. Chem. Soc.* 2019, **141**, 13948.

14 M. J. T. Frisch, G. W, H. B. Schlegel, G. E. Scuseria, M. A. Robb, J. R. Cheeseman, G. Scalmani, V. Barone, G. A. Petersson, H. Nakatsuji, X. Li, M. Caricato, A. V. Marenich, J. Bloino, B. G. Janesko, R. Gomperts, B. Mennucci, H. P. Hratchian, J. V. Ortiz, A. F. Izmaylov, J. L. Sonnenberg, D. Williams-Young, F. Ding, F. Lipparini, F. Egidi, J. Goings, B. Peng, A. Petrone, T. Henderson, D. Ranasinghe, V. G. Zakrzewski, J. Gao, N. Rega, G. Zheng, W. Liang, M. Hada, M. Ehara, K. Toyota, R. Fukuda, J. Hasegawa, M. Ishida, T. Nakajima, Y. Honda, O. Kitao, H. Nakai, T. Vreven, K. Throssell, J. A. Jr. Montgomery, J. E. Peralta, F. Ogliaro, M. J. Bearpark, J. J. Heyd, E. N. Brothers, K. N. Kudin, V. N. Staroverov, T. A. Keith, R. Kobayashi, J. Normand, K. Raghavachari, A. P. Rendell, J. C. Burant, S. S. Iyengar, J. Tomasi, M. Cossi, J. M. Millam, M. Klene, C. Adamo, R. Cammi, J. W. Ochterski, R. L. Martin, K. Morokuma, O. Farkas, J. B. Foresman and D. J. Fox, *Gaussian 16 Revision C. 01*, 2016, **1**, 572.

15 H. Luo, Z. Gao, H. Muwanwella, G. Sanfo, Y. Lu, S. Yang, Y. Ren, S. Hou, X. Liu, P. K. Sharma, R. Palgrave, M. T. Sajjad, P. Huang and M. Abdi-Jalebi, *Small* 2025, e07718.

16 H. Tan, X. Yu, W. Ren, T. Yin, H. Wen, Y. Guo, Z. Zhang, C. Liu, G. Zhou, H. Li, X. Qiu, H. Wu, Z. Yang and S. Huang, *Small* 2025, **21**, 2500978.

17 Y. Gao, W. Gong, Z. Zhang, J. Guo, J. Ma, X. Li, Y. Zeng and M. Wu, *Angew. Chem. Int. Ed.* 2025, **64**, e202424479.

18 L. Sun, T. Wang, Y. Wang, G. Li, Z. Deng, S. Sun, H. Tan, X. Wang, J. Chen, L. Peng, X. Liu, J. Lin and H. Li, *Adv. Energy*

Mater. 2025, **15**, 2405581.

19 Y. Wu, Y. Wang, J. Song, X. Wu, Y. Zhao, H. Li, X. Yin, L. Hu, Z. Su, Y. Jin, X. Zhang, Y. Cheng and Z. Li, *Appl. Phy. Lett.* 2024, **124.**

20 Y. Li, J. Chen, X. Chen, W. Meng, D. Wang, S. Zhang, H. Zhong, C. Yao and Q. Zhang, *Chem. Eng. J.* 2025, **518**, 164637.

21 C. Hao, R. Xu, B. Li, Y. Chen, Q. Jia, Z. Wang, J. Pei, B. Zhang, Y. Su, J. Li and H. Dong, *Angew. Chem. Int. Ed.* 2025, **137**, e202508169

22 Y. Zang, Y. Tu, C. Jiao, W. Li, P. Zhou, J. Cheng, G. Yang, T. Shao, J. Ye, G. Li, L. Chu, S. Lu, G. Liang, Y. Liang, J. Wang, Z. Zhong, R. Hu and W. Yan, *Chem. Eng. J.* 2024, **480**, 148133.

23 K. Sun, Z. Wang, N. Li, L. Liu, W. Xiong, Z. Xu, Z. Geng, X. Guo, Y. Jiang, S.-P. Feng, X. Gao, Y. Chen, J. Liu and J. Gao, *Adv. Mater.* 2025, **37**, 2419419.

24 X. Chen, Z. Jia, Z. Chen, C. Zhou, S. Huang, X. Xia, S. Liang, P. Wang, T. Jiang, T. Liu, X. Xu, B. Yan, J. Yao, X. Lu, W. Shen, H. Zhu and Y. Yang, *Adv. Mater.* 2025, **37**, 2500190.

25 Z. Wang, Y. Liu, F. Zhao, W. Yang, S. Deng, C. Li, J. Cao, W. An, J. Pan and L. Shi, *Appl. Phys. Lett.* 2025, **127**, 6.

26 B. J. Kim, G. Seo, S. Park, D. Lee, Y. Luo, S. Wieghold, M.-c. Kim and G. Boschloo, *J. Mater. Chem. A* 2024, **12**, 33870.

27 H.-C. Hsu, J.-C. Tsao, C.-H. Yeh, H.-T. Wu, C.-T. Wu, S.-H. Wu, and C.-F. Shih, *Nanomaterials*, 2024, **14**, 1315.

28 G. Y. Park, M.-J. Kim, J. Y. Oh, H. Kim, B. Kang, S.-K. Cho, W. J. Choi, M. Kim and D. S. Ham, *ACS Appl. Mater. Interfaces* 2024, **16**, 27410.

29 C.-F. Li, S.-H. Huang, Y.-R. Chen, H.-C. Cha, S.-Y. Chung, Y.-H. Hsiao, F.-Y. Tsai and Y.-C. Huang, *Chem. Eng. J.* 2025, **517**, 164194.

30 N. K. Rana, D. P. Singh and N. Chander, *ACS Appl. Electron. Mater.* 2024, **6**, 3325.

31 F. Ansari, L. Zheng 1, L. Pfeifer 1, F. T. Eickemeyer, S. Zakeeruddin, N. Lempesis, V. Carnevali, A. Vezzosi, V. Sláma, T. Georges, U. Gunes, L. Emsley, M. Nazeeruddin, U. Rothlisberger, P. J. Dyson and M. Grätzel*, Adv. Mater.* 2025, **37**, 2501075.

32 C. Wang, Y. Mo, X. Gao, Q. Huang, T. Bu, Q. Li, Y. Cheng and F. Huang, *Sci. Adv.* 2025, **11**, eadu1116.

33 D. Yang, R. Yang, C. Zhang, T. Ye, K. Wang, Y. Hou, L. Zheng, S. Priya, S. Liu, *Adv. Mater.* 2023, **35**, 2302484.

34 P. Liu, H. Wang, T. Niu, L. Yin, Y. Du, L. Lang, Z. Zhang, Y. Tu, X. Liu, X. Chen, S. Wang, N. Wu, R. Qin, L. Wang, S. Yang, C. Zhang, X. Pan, S. Liu, K. Zhao, *Energy Environ. Sci.* 2024, **17**, 7069.

35 F. Jafarzadeh, L. A. Castriotta, F. De Rossi, J. Ali, F. Di Giacomo, A. Di Carlo, F. Matteocci, F. Brunetti, *Sustain. Energy Fuels.* 2023, **7**, 2219.

36 B. Taheri, F. De Rossi, G. Lucarelli, L. A. Castriotta, A. Di Carlo, T. M. Brown, F. Brunetti, *ACS Appl. Energy Mater.* 2021, **4**, 4507.

37 L. Dong, S. Qiu, J. García Cerrillo, M. Wagner, O. Kasian, S. Feroze, D. Jang, C. Li, V. M. Le Corre, K. Zhang, H. Peisert, F. U. Kosasih, C. Ducati, C. Arrive, T. Du, F. Yang, C. J. Brabec, H.-J. Egelhaaf, *Energy Environ. Sci.* 2024, **17**, 7097.

38 H. C. Weerasinghe, N. Macadam, J.-E. Kim, L. J. Sutherland, D. Angmo, L. W. T. Ng, A. D. Scully, F. Glenn, R. Chantler, N. L. Chang, M. Dehghanimadvar, L. Shi, A. W. Y. Ho-Baillie, R. Egan, A. S. R. Chesman, M. Gao, J. J. Jasieniak, T. Hasan, D. Vak, *Nat. Commun.* 2024, **15**, 1656.